Chapter 20

A Novel Hypoxia Imaging Endoscopy System

Kazuhiro Kaneko, Hiroshi Yamaguchi and Tomonori Yano

Additional information is available at the end of the chapter

http://dx.doi.org/10.5772/66091

Abstract

Measurement of tumor hypoxia is required for the diagnosis of tumor and the evaluation of therapeutic outcome. Currently, invasive and noninvasive techniques being exploited for tumor hypoxia measurement include polarographic needle electrodes, immunohistochemical (IHC) staining, magnetic resonance imaging (MRI), radionuclide imaging (positron emission tomography [PET] and single-photon emission computed tomography [SPECT]), optical imaging (bioluminescence and fluorescence), and hypoxia imaging endoscopy. This review provides a summary of the modalities available for assessment of tissue oxygenation as well as a discussion of current arguments for and against each modality, with a particular focus on noninvasive hypoxia imaging with emerging agents and new imaging technologies intended to detect molecular events associated with tumor hypoxia.

Keywords: Hypoxia imaging endoscopy, innovation of endoscopy

1. Introduction

In the 1950s, hypoxia research began, and many clinical trials have been reported. Hypoxia of tumor affects outcomes after radiotherapy. But hypoxia has also been shown to be a poor prognostic factor after chemotherapy and surgery. These findings are attributed to chronic hypoxia. Hypoxic tumors are more likely to recur loco-regionally than well-oxygenated tumors regardless of whether surgery or radiation therapy is the primary local treatment. However, the common oxygen measurement used in these reports was polarographic needle electrodes inserted directly into specific sections of tumor tissue. In this method, hypoxia was measured in only pinpointed area for the tumor. In other words, there was no modality used

in which the hypoxia imaging results were visible in real time and which reflected the hypoxic state in the whole tumor. Therefore, hypoxia imaging is expected to allow direct visualization of the biological and functional changes in cancer.

Hypoxia is a histopathological condition in which cells in tissues suffer from lack of oxygen for their normal metabolism. An oxygen saturation (StO_2) of arterial blood is almost 100% and that of venous blood is approximately 70%. In contrast, the StO_2 in half of cancers is 50–60% at the highest. Hypoxia takes hold as a tumor becomes large enough to disrupt the balance of oxygen supply and consumption in the area. Approximately, 50–60% of advanced cancer forming solid tumor may show hypoxic and/or anoxic conditions exhibiting heterogeneous distribution in the inside of tumor [1]. Hypoxia proliferates rapidly in solid tumors, and their intratumoral vessels with significantly structural abnormalities are distributed spatially with dilated, tortuous, saccular, and heterogeneous figures. As a result, this distribution leads to perfusion-limited delivery of O_2 [2]. There are mainly two types of hypoxia regarding solid tumor and tissue around tumor. One is perfusion-limited O_2 delivery type, the so-called acute hypoxia, which leads to ischemic condition, however, it is often transient. Another type is diffusion-limited hypoxia, the so-called chronic hypoxia, which can also be caused by an increase in diffusion distances, so that cells far away (>70 μm) from a nutritive blood vessel receive less oxygen (and nutrients) than needed [1]. Regarding hypoxia-induced proteome and/or genome changes, cell cycle arrest, differentiation, apoptosis, and necrosis are found in solid tumor. In contrast, hypoxia-induced changes of proteome may progress tumor growth because of mechanisms enabling cells to overcome nutritive deprivation, to escape from the hostile environment and to favor unrestricted growth. Furthermore, continuous hypoxia can also bring cellular changes as a more aggressive phenotype [3]. Since the presence of hypoxic status in solid tumors was first reported in 1953 to be among the factors associated with treatment failure following radiation therapy [4], tumor hypoxia has drawn attention as a pivotal event in tumor invasion, angiogenesis, apoptosis, metastasis [1], resistance to chemotherapy [5], surgery, and resistance to radiotherapy [6]. In tumor diagnosis and treatment planning, it is crucial to have a grasp of the degree and extent of tumor hypoxia involved prior to the start of treatment.

2. Clinical importance for measurement of tumor hypoxic state

A variety of techniques are being proposed to assess tumor hypoxia, which can be broadly categorized into direct measurements and indirect measurements according to different principles and the ability to quantify tissue oxygenation. Direct measurements, including polarographic needle electrode, phosphorescence imaging, near-infrared spectroscopy (NIRS), blood oxygen level dependent (BOLD) and ^{19}F magnetic resonance imaging (MRI) and electron paramagnetic resonance (EPR) imaging, can detect oxygen partial pressure (pO_2), oxygen concentration, or oxygen percentage. Recently, a hypoxia imaging endoscopy that can derive the oxygen saturation (StO_2) was developed in endoscopic fields. Indirect measurements, including measuring exogenous and endogenous hypoxia markers, can provide parameters related to oxygenation.

http://dx.doi.org/10.5772/66091

Many clinical trials have been performed using direct and indirect measurement methods. It is now known that hypoxia affects outcome after radiotherapy, with poor prognosis in hypoxic cancers. Next, hypoxia has also been shown to be a poor prognostic factor after chemotherapy and surgery. Furthermore, hypoxic tumors are more likely to recur loco-regionally than well-oxygenated tumors regardless of whether surgery or radiation therapy was the primary local treatment.

3. Direct measurements for hypoxia

3.1. Polarographic needle electrodes for direct tumor tissue

The invasive polarographic needle electrodes have been widely employed since the 1990s to assess tumor oxygen status and to measure pO_2 in both human and animal studies [7, 8]. As the gold standard modality, their use has been extended not only to lymph node metastases but to more accessible tumors, which include head and neck cancer, cervical cancer, soft tissue sarcomas of the extremities, astrocytic brain tumors, lung cancer, pancreatic cancer, prostate cancer, and lymph node metastases [8–12]. With the average median pO_2 before treatment of 11.2 mmHg (range 0.4–60 mmHg) [7], these measured values help prediction of the tumor response to treatment [13] and tumor metastatic potential [14]. The polarographic needle electrode is currently available under CT guidance for evaluating tumor pO_2 in deep-seated organs as well as for assessing overall tumor oxygen status [15] with the caveat, however, that insertion of an electrode into the tumor leads to disruption of tissues, thus rendering it difficult to distinguish the necrotic areas and to establish the patterns of hypoxia involved. Furthermore, the use of the modality not only calls for great expertise but is associated with large interobserver variability.

4. Noninvasive imaging of hypoxia

While the polarographic needle electrode and immunohistochemical (IHC) staining can provide a relatively accurate estimation of tumor oxygenation, being subject to selection bias, provide only a partial, but not complete, picture of the entire tumor site [16]. This has led to an increasing interest in the use of noninvasive functional and molecular imaging modalities, which is capable of yielding a large amount of high-quality experimental data per protocol by increasing the number of quantitative data collections and by guiding tissue sampling and allowing a rapid and effective combination of analyses to be conducted [17].

Several imaging modalities have been developed, to date, to allow direct or indirect measurement of tumor oxygenation, with a few of these remaining less mature for clinical application. Of these, EPR spectroscopy, which involves the use of unpaired electron species to obtain images and spectra, is currently being explored in animals as a means to provide a quantitative measure of tissue oxygenation [18]. Although this modality has considerable potential to be developed as a tumor oximeter, i.e., in monitoring changes after tumor oxygenation [19], a

suitable paramagnetic marker with low toxicity for human remains yet to become available. The need for appropriate EPR instrumentation in the clinical setting also prevents this promising modality from becoming widespread [20]. Photoacoustic tomography (PAT) is also available for imaging blood oxygenation using the differential optical contrast between O_2Hb and dHb. PAT has been implemented for imaging cerebral blood oxygenation of rats *in vivo*, demonstrating that PAT is capable of capturing the changes from hyperoxia to hypoxia [21], while no study reported on its clinical application.

4.1. Magnetic resonance imaging

BOLD-MRI is shown to have potential as a diagnostic modality for tumor hypoxia [22]. Hemoglobin occurs as deoxyhemoglobin in oxygen-deficient states, where not oxyhemoglobin but paramagnetic deoxyhemoglobin can increase the transverse relaxation of the surrounding protons [23]. BOLD-MRI employs deoxyhemoglobin-derived endogenous signals as image contrast to depict changes in oxygenation in blood. Decreased oxygenation in blood results in decreased signal intensity in T2-weighted images, and this correlation between the BOLD-MRI signal and vascular oxygenation allows pO_2 to be directly estimated. This has indeed led to numerous studies being conducted to investigate carbogen breathing in mice, oxygenation in tumor models [24], and kidney function in patients [22, 25, 26] using the modality as a noninvasive technique with high spatial and temporal resolution [22]. As with phosphorescence and near-infrared fluorescence imaging, the major disadvantage of BOLD-MRI is that it reflects change in oxygen tension in vasculature but not those in tissues. Again, not being a quantitative method, it may easily be affected by multiple factors such as flow effects, hematocrit, pH, and temperature [27].

^{19}F MRI involves the use of two types of markers, i.e., perfluorocarbons (PFCs) and fluorinated nitroimidazoles as contrast agents, which are not used in conventional T1-weighted MRI. While being highly hydrophobic, PFCs are highly oxygen soluble [28]. Due to the linear relationship between the ^{19}F spin lattice relaxation rate of PFCs and the dissolved oxygen concentration, the ^{19}F-based oximetry allows vascular oxygenation to be measured *in vivo* [29]. PFCs investigated to date include hexafluorobenzene (HFB) [30] and perfluoro-15-crown-5-ether (PF15C5) [31, 32], which are injectable intravenously or intratumorally. ^{19}F MRI is increasingly employed to detect changes in tumor oxygenation that occur in response to treatments that are radio-sensitizing and oxygen-augmenting [33]. The disadvantages of ^{19}F MRI are that flow artifacts affect the measurements and that, with some contrast agents, oxygen sensitivity is easily influenced by such conditions as temperature, dilution, pH, common proteins, and blood [34]. Following intravenous injection, most PFC contrast agent is extensively ingested by the reticuloendothelial system (RES) and their slow clearance may cause adverse reactions. Their intratumoral injection may also raise concern over its associated risk, e.g., embolism associated with accidental injection of PFC emulsion into the tumoral vein [35]. One major drawback of the nitroimidazole derivatives is their central nervous system (CNS) toxicity profile, with misonidazole shown to be associated with neuropathy and acute toxicity on the CNS [33].

"Vessel architectural imaging" (VAI) has recently been proposed as a new paradigm in MRI providing a basis for vessel caliber estimation [36] by incorporating an overlooked temporal shift in the MR signal, thus generating, unlike any other noninvasive imaging modality, new information on vessel type and function. Indeed, this new modality allowed an oral pan-vascular endothelial growth factor (pan-VEGF) receptor kinase inhibitor to be evaluated for its therapeutic efficacy in glioblastoma patients [37], demonstrating using VAI that anti-VEGF therapy not only normalizes tumor vasculature and alleviates edema but also prolongs survival in these patients.

4.2. Positron emission tomography

Efforts have recently been directed toward developing contrast agents for noninvasive hypoxia imaging with positron emission tomography (PET) and single-photon emission computed tomography (SPECT). Organic molecular markers labeled with positron-emitting radioisotopes are employed in PET imaging to allow the extent of tumor hypoxia to be measured. Commonly used radioisotopes include ^{18}F, ^{124}I, and $^{60/64}$Cu and the molecular markers to be labeled with these isotopes include 2-nitroimidazoles, e.g., fluoromisonidazole (FMISO), EF5, and fluoroetanidazole (FETA), nucleoside conjugates, e.g., iodoazomycin arabinoside (IAZA), and Cu(II)-diacetyl-bis (N4-methylthiosemicarbazone) (Cu-ATSM) [38–40]. These markers are shown not only to bind maximally to severely hypoxic cells to form such stable adducts as are detectable with a PET scanner but to provide a clear demarcation of hypoxic cells *in vivo* through their rapid reoxidization and removal from normal cells.

Of the first-generation nitroimidazoles, ^{18}F-labeled misonidazole (^{18}F-FMISO) is the most commonly used as being sensitive only to the presence of hypoxia in viable cells [41]. It is reported that a hypoxic state defined as <10 mmHg is required to induce significant ^{18}FMISO uptake [42]. ^{18}F-FMISO uptake is shown to vary widely depending on the type of patients and tumors, whereas ^{18} F-FMISO is shown to allow hypoxia to be detected in various tumors such as glioma, head and neck cancer, renal tumor, and non-small cell lung cancer [42–44]. A clinical trial of glioblastoma multiforme patients [45] demonstrated increased ^{18}F-FMISO uptake and retention on both post-treatment FMISO and FDG images, suggesting that reoxygenation did not take place. It is reported that the distribution of oxygen and hypoxia was increased and decreased, respectively, in non-small cell lung carcinomas following treatment, as assessed by sequential FMISO imaging [46]. Given that no correlation is shown between patient diagnosis and degree of decrease in FMISO uptake and retention, in selectively boosting the radiation dose to hypoxic subvolumes, there appears to be a larger role for serial imaging during treatment than for baseline volume measurement. Again, pretreatment FMISO uptake/retention and survival has been shown to be correlated and allow treatment failure to be predicted [45, 47]. However, ^{18}F-FMISO may not be readily available for use in other cancers [42, 48].

The second-generation nitroimidazoles include 18F-fluorerythronitroimidazole (FETNIM) [49, 50], FETA [51], and EF5 [52, 53], which are more water soluble and not readily susceptible to degradation by most oxidizing mechanisms in place in humans. ^{18}F-EF5 was tested in clinical trials for its feasibility as an imaging agent for hypoxia [54] and was shown to be

hypoxia-specific, with its increased uptake shown to be correlated with the extent of tumor and high risk of metastasis in cancer patients [52], suggesting its usefulness in identifying high-risk candidates for clinical trials evaluating the influence of early chemotherapy on the occurrence of metastasis [55]. ^{18}F-FAZA has great promise as an imaging agent for tumor hypoxia due to its faster diffusion into cells and faster clearance from normal tissues than ^{18}F-FMISO [56]. PET imaging using ^{18}F-FMISO demonstrated very high tracer uptake in all seven patients with high-grade gliomas evaluated, showing the potential of ^{18}F-FMISO as an imaging agent in assessing hypoxia in this tumor type [57].

4.3. Phosphorescence imaging

Phosphorescence imaging with injection of porphyrin complex (Oxyphor) into the vasculature also allows tumor vascular pO_2 to be measured [58, 59]. Recently, a general approach has been proposed through which to construct phosphorescent nanosensors with tunable spectral characteristics, varying degrees of quenching, and a high oxygen selectivity [60]. These probes are shown to exhibit excellent performance in measuring vascular pO_2 in the rat brain with *in vivo* microscopy [60]. NIRS are also available for analysis of tumor oxygenation *in vivo* based on recorded spectral changes by hemoglobin in the vasculature [61–63]. Kim and Liu [64] demonstrated in an animal study that NIRS is associated with comparable efficacy to that with electrode measurements in evaluating tumor hypoxia. They showed that either carbogen (95% CO_2 and 5% O_2) or 100% oxygen inhalation could improve the vascular oxygen level of rat breast tumors. However, both phosphorescence imaging and NIRS are not readily translatable into clinical applications due to their low spatial resolution, light scattering, limited path length, low sensitivity, and susceptibility to environmental influence.

4.4. Visible light spectroscopy

In the search for noninvasive, continuous modalities for monitoring ischemia, electrical bioimpedance cardiac output monitoring has been proposed but shown to be incompatible with the thermodilution methods [65, 66]. Again, while near-infrared spectroscopy (NIRS) [67] is shown to respond to both hypoxemia [68, 69] and ischemia [70–72], its clinical use has been limited to large organs, such as the brain [73, 74, 85–87] with its broad normal ranges reported to be between 48% and 88% [75, 76]. Similarly, wide normal ranges are reported for sublingual capnography [77–79]. Also available, albeit invasive are polarographic oximetry probes [80] and fiber-enabled pulmonary catheters.

Visible light spectroscopy (VLS) appears to be similar to NIRS on some counts [81] with its mean VLS StO2 shown to be not significantly different from NIRS StO2 reported in human studies [67–76]. Again, the fractional contribution of venous blood to the cerebral NIRS signal has been reported to be 0.84 ± 0.21 ranging from 0.60 to 1.00 [82–84]. Using central venous and pulse oximetry saturation as estimates for local venous and arterial saturation, it is shown to be not significantly different at 0.89 ± 0.04. It is suggested that the two modalities cover similar microvascular compartments.

At the same time, VLS is shown to be superior to NIRS in monitoring tissues that lend themselves to monitoring, thus suggesting a more versatile role for VLS in patient treatment [81]. The NIRS light sources and detectors require to be spaced 2–5 cm apart or more to illuminate and monitor a large, homogenous tissue volume (>30 ml), thus making NIRS with its long and bulky sensors unsuitable for monitoring tissue regions, e.g., thin tissues such as gastrointestinal mucosa or small tumors. In contrast, the visible light used in VLS is shown to be strongly absorbed by tissue and VLS measurement to be highly localized thus making VLS unsuitable for transcranial use or use over thick skin dominated by surface tissue properties. Using VLS, a rapid real-time drop in tumor oxygenation was detected during local ischemia following clamping or epinephrine administration [85], with the tissue oximetry performed during endoscopy demonstrating a significantly lower tissue oxygenation (StO_2) in tumors (46% ± 22%) than in normal mucosa (72% ± 4%) ($P < 0.0001$). Thus, VSL tissue oximetry may be able to distinguish neoplastic tissue with a high specificity to aid in the endoscopic detection of gastrointestinal tumors. Again, of note, chronic gastrointestinal ischemia was also detected using the same method [86] (**Figure 1**).

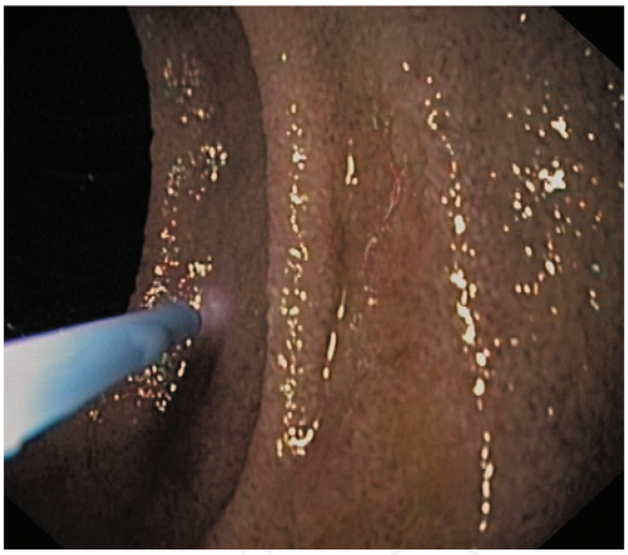

Figure 1. VLS measurements using a fiber-optic catheter-based VLS oximeter. The catheter is passed through the accessory channel of the endoscope and positioned about 1–5 mm above the mucosa.

5. Hypoxia imaging endoscopy with no phosphor

Kaneko et al. [87] reported hypoxia imaging endoscopy equipped with a laser light source. In this system, signals from the laser light passed through the processor were calculated as StO_2. The measurement range of StO_2 was from 0% to 100% in contactless of tumor or normal mucosa under endoscopic observation. Display imaging was performed with the use of laser light alone without phosphor, provided a display of overlay and pseudocolor images. The laser light used was not near-infrared but ranged within visible light wavelengths. In principle, this utilized

the difference in absorption coefficient between oxyhemoglobin and deoxyhemoglobin. Two challenges were identified, however, in deriving the StO_2 of tissue in alimentary tracts from differences in absorption spectra between oxyhemoglobin and deoxyhemoglobin using small numbers of wavelengths. First, there is not only a small difference in optical absorption spectra in the visible light region but also a narrow bandwidth between isosbestic points. Second, the reflectance of a tissue depends on hematocrit (Hct) as well as StO_2, given that light absorption increases as hemoglobin density increases.

An imaging system equipped with laser diodes of 445 and 473 nm and a white fluorescent pigment body was therefore developed. Hypoxia imaging with this system rendered visible an alimentary tract tumor in real time and allowed the whole tumor to be visualized. With the tumor surface and normal mucosa rendered visible, no heterogeneity was seen with the use of this system. In the first-in-human clinical trial, early cancers of the esophagus, stomach, and colorectum were detected as hypoxic areas (**Figure 2**). Furthermore, colorectal adenomas with histologically low-grade atypia were also detected as hypoxic areas and no complications were reported in the patients with visualization of these tumors in real-time hypoxia imaging which involved only laser light without injection or oral administration of phosphor. As mentioned above, it will be expected that the hypoxia imaging endoscopy is shown to be superior to VLS or NIRS in measuring StO_2 of surface of tumor and normal mucosa.

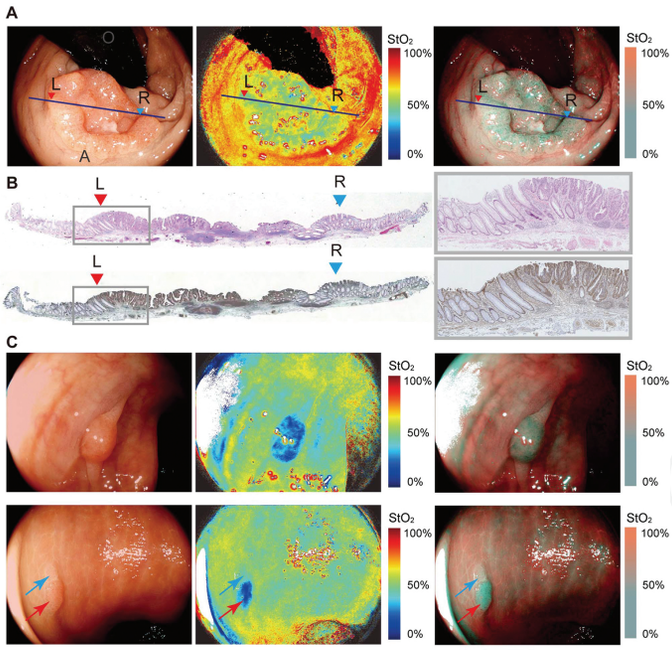

Figure 2. StO_2 maps obtained in human subject research. (A) White light image by endoscopic observation in rectal adenocarcinoma (left). Line (L-R) corresponds to cross section of pathological diagnosis. StO_2 map visualized by laser endoscope system (middle: pseudocolor StO_2 image; right: StO_2 overlay image). (B) Cross-sectional appearance stained with H&E (upper) and HIF1 alpha antibody (lower) corresponding to the hypoxic area visualized with StO_2 map. (C) Endoscopic images of a colorectal adenoma (upper) showing clear hypoxia: white light image (upper left), pseudocolor StO_2 map (upper middle) and overlayed image (upper right). Another case of a colonic lesion (lower) consisting of an adenoma (red arrow) and a hyperplasia (blue arrow): white light image (lower left), pseudocolor StO_2 map (lower middle) and overlayed image (lower right). Only the adenoma was detected as hypoxia.

6. Indirect hypoxia evaluation

Proteins and genes whose expression is associated with hypoxia have potential as endogenous molecular markers of hypoxia and have been explored over the years; meanwhile, hypoxia-specific agents have also been explored and shown to be useful in monitoring hypoxia [88]. Immunohistochemical (IHC) staining for hypoxia marker adducts in situ is also available to provide indirect quantitative information on the relative oxygenation of tissue at a cellular resolution. IHC approaches have a role to play particularly *in vitro* studies, including assays of human biopsy specimens. Given the complex biology of tumor hypoxia for which no single marker is expected to have a strong prognostic power in clinical practice, efforts have been directed toward combining various markers to create a prognostic profile of hypoxia [89].

6.1. Hypoxia-inducible factor 1

Optical imaging has had an important role to play in evaluating hypoxia, especially in biopsy specimens. With the introduction of transgenes with the hypoxia responsive element as promoter sequences coupled to reporter genes, e.g., luciferase reporter gene [90, 91] or green fluorescent protein (GFP) [92], a number of modalities have been developed to allow HIF-1 activity to be directly measured. Of these, a HIF-1-dependent promoter-regulated luciferase reporter gene, shown to produce a 100-fold increased luciferase response to hypoxia, has been used to evaluate anti-hypoxia therapy for its efficacy in animals [93]. Again, an imaging probe has been developed for HIF-1-active cells using a PTD-ODD fusion protein. given that, being involved in the same ODD control as HIF-1α, PTD-ODD fusion proteins are thought likely to be co-localized with HIF-1α [93–96]. First developed as a model probe, PTD-ODD-enhanced GFP-labeled with near-infrared fluorescent dye Cy5.5 was shown to permeate cell membrane with high efficiency, with its stability controlled in an oxygen concentration-dependent manner; to accumulate in hypoxic tumor cells with HIF-1 activity, thus allowing the hypoxic tumor cells with HIF-1 activity to be imaged in contrast to the surrounding cells under aerobic conditions [96]. Bioluminescence imaging has also been used to noninvasively depict HIF-1α as it is upregulated *in vivo* following chemotherapy, suggesting that this modality may prove useful in the evaluation of emerging anti-HIF-1 therapeutics [97]. While these imaging tools have a role to play in elucidating the biology of hypoxia and mechanisms of tumor response to therapy, heterogeneous gene responses to HIF-1 pose challenges to these HIF-1-targeted modalities. Furthermore, only weak correlation has been shown between HIF-1α expression and oxygen electrode or PET imaging measurements [98, 99], thus throwing in doubt the value of HIF-1α quantification as a measure of hypoxia.

6.2. Carbonic anhydrase IX

Downstream of HIF-1, carbonic anhydrase 9 (CA IX), a member of the CA family known to exist in cytosolic, membrane-associated, mitochondrial, and secreted carbonic anhydrases (CAs), may represent an alternative target [100]. A membrane-associated enzyme involved in the respiratory gas exchange and acid-base balance, CA IX is shown to be found less

abundantly in normal tissue and only in gastric mucosa, small intestine, and muscle. Under hypoxic conditions, CA IX is shown to be overexpressed in different types of cancer [101], with the staining pattern shown to be more generalized in VHL-associated tumors and focal-perinecrotic in non-VHL-associated tumors [102].

CA IX has been imaged with fluorescent-labeled sulfonamides in a tumor xenograft model to allow hypoxic and (re)-oxygenated cells to be distinguished [103], which demonstrated that CA IX required exposure to hypoxia for its binding and retention—a finding confirmed by an *in vivo* imaging study [103]. In renal-cell carcinoma xenografts, a G250 monoclonal antibody against CA IX was shown to significantly inhibit tumor growth [104]. Again, phase II clinical trials employed G250-based radioimmunoimaging to detect primary and metastatic lesions as well as to guide radioimmunotherapy after labeling G250 with therapeutic radioisotopes, which included ^{177}Lu, ^{90}Y, or ^{186}Re [105]. High-affinity human monoclonal antibodies (A3 and CC7) specific to human CA IX were developed using phage display technology [106] and these reagents may have a role to play in a wide range of settings, including noninvasive imaging of hypoxia and drug delivery [106]. In this regard, combining CA IX and a proliferation marker may prove helpful in identifying proliferating cells under hypoxic conditions [107, 108], while no correlation is shown between the amount of CA IX and direct oxygen measurement with a needle electrode [109].

Furthermore, hypoxia markers have been identified and shown to be induced by hypoxia and expressed in human tumors, including VEGF and GLUTs, both of which are upregulated by increased activity of HIF-1 under hypoxic conditions [110]. Imaging strategies targeting these proteins have also been explored for their ability to assess tumor vasculature and proliferation, while the relationship between pO_2 values and protein expression levels remains unclear [111].

7. Heterogeneity of tumor

Tissue oxygenation is shown to be highly heterogeneous due to the presence of both highly oxygenated arterial vascular regions and poorly oxygenated tissues and cells. Spatial and temporal heterogeneity also contribute to the complexity of the issue. Heterogeneity is thus a major factor in hypoxia measurement that affects our ability to stratify patients and predict outcomes using the imaging technologies available, and its biological implications need to be further explored, and effective approaches to assessing heterogeneity remain to be established. Hypoxia imaging endoscopy allowed early cancers of the pharynx, esophagus, stomach, and colorectum to be captured in whole for the first time [87], with no heterogeneity found in nearly all early cancers or colorectal neoplasia detected. Given that tissue heterogeneity may vary between early, advanced, and metastatic tumors, however, it remains crucial to elucidate tissue heterogeneity as it is associated with tumor progression.

8. Future of hypoxia measuring methods

Given the wide variety of techniques available for assessing hypoxia, e.g., polarographic needle electrodes, IHC staining, PET, MRI, optical imaging with NIR fluorescence or bioluminescence, visible light spectroscopy, and hypoxia imaging endoscopy, it remains critically important to determine their relative advantages and disadvantages for clinical application. Improvements in hypoxia measuring techniques will hinge primarily on which techniques are chosen and how these techniques are applied in the clinic. Clearly, the best of these are expected to be sensitive to the biological sequel of hypoxia, and the ideal one expected to be clinically safe, readily available, minimally invasive, and free from radiation exposure, while at the same time providing high resolution and ease of use. In addition, NIR over 1000 nm wavelength, the so-called biological window, will be promising, because this wavelength area is good for tissue permeability due to reducing both light scattering and infrared absorption [112].

In the endoscopic fields of alimentary tracts, the existing diagnosis for neoplasia is based on the morphologic features of the tumor. However, imaging of a tumor focused on its function or metabolism yields a novel set of data. Hypoxia imaging endoscope system equipped with a laser source allows oxygen saturation to be shown with two types of overlay and pseudocolor images displayed one on top of the other [87]. Available for handling similarly to conventional endoscopy, this modality is easy to treat with and completely safe without being invasive. Of the large number of patients with cancers in the alimentary tract, such as oral cavity, esophagus, stomach, and colorectum in the world, a majority with advanced cancer patients receives chemotherapy, radiotherapy, and combination therapy. In this regard, this modality is expected to allow not only hypoxic states but also hyperoxic states of tumor to be detected in these patients, thus contributing to selection of therapy or drug as well as evaluation of their therapeutic efficacy. Furthermore, this modality will serve as a screening method facilitating detection of early cancer. Advances in research into hypoxia and intratumoral microvessels of tumor with this endoscopic modality are expected and lead to development of new drugs. Thus, the proposed laser source-equipped hypoxia endoscope system appears to have the potential to redraw the endoscopic landscape.

9. Conclusions and perspectives

Tumor hypoxia assessment allows cancer patients to be followed up early after treatment initiation and drug resistance and radioresistance to be predicted. Current insights into the molecular mechanisms of hypoxia have indeed led to novel probes being developed for noninvasive imaging of hypoxia. Again, real-time hypoxic imaging in digestive endoscopy was obtained using such laser light as remains within visible light wavelengths, with no use of any probes. For innovation of endoscopy, it was elucidated that most of all early cancers and precursor lesions have already been to hypoxic state. This is a cutting edge finding. This imaging technology highlights a novel aspect of cancer biology as a potential biomarker which

may come to be widely used in cancer diagnosis and treatment effect prediction. These approaches appear to have great promise and further studies on the predictive value of hypoxia measurement in tumors may help identify independent predictive marker of hypoxia as well as optimal parameters for assessing hypoxia. It remains to be clarified whether these new agents may help reduce hypoxic disease or whether they are available for hypoxia imaging.

Author details

Kazuhiro Kaneko[1], Hiroshi Yamaguchi[2] and Tomonori Yano[1*]

*Address all correspondence to: toyano@east.ncc.go.jp

1 Division of Science and Technology for Endoscopy, National Cancer Center Hospital East, Chiba, Japan

2 Imaging Technology Center, FUJIFILM Corporation, Tokyo, Japan

References

[1] Vaupel P, Mayer A (2007) Hypoxia in cancer: significance and impact on clinical outcome. Cancer Metastasis Rev 26:225–239

[2] Fukumura D, Jain RK (2007) Tumor microvasculature and microenvironment: targets for anti-angiogenesis and normalization. Microvasc Res 74:72–84

[3] Vaupel P, Mayer A, Hockel M (2004) Tumor hypoxia and malignant progression. Methods Enzymol 381:335–354

[4] Gray LH, Conger AD, Ebert M, Hornsey S, Scott OCA (1953) The concentration of oxygen dissolved in tissues at the time of irradiation as a factor in radiotherapy. Br J Radiol 26:638–648

[5] Matthews NE, Adams MA, Maxwell LR, Gofton TE, Graham CH (2001) Nitric oxide-mediated regulation of chemosensitivity in cancer cells. J Natl Cancer Inst 93:1879–1885

[6] Nordsmark M, Bentzen SM, Rudat V et al (2005) Prognostic value of tumor oxygenation in 397 head and neck tumors after primary radiation therapy. An international multi-center study. Radiother Oncol 77:18–24

[7] Brizel DM, Sibley GS, Prosnitz LR, Scher RL, Dewhirst MW (1997) Tumor hypoxia adversely affects the prognosis of carcinoma of the head and neck. Int J Radiat Oncol Biol Phys 38:285–289

[8] Hockel M, Vorndran B, Schlenger K, Baussmann E, Knapstein PG (1993) Tumor oxygenation: a new predictive parameter in locally advanced cancer of the uterine cervix. Gynecol Oncol 51:141–149

[9] Nordsmark M, Loncaster J, Chou SC et al (2001) Invasive oxygen measurements and pimonidazole labeling in human cervix carcinoma. Int J Radiat Oncol Biol Phys 49:581–586

[10] Nordsmark M, Overgaard J (2000) A confirmatory prognostic study on oxygenation status and loco-regional control in advanced head and neck squamous cell carcinoma treated by radiation therapy. Radiother Oncol 57:39–43

[11] Evans SM, Judy KD, Dunphy I et al (2004) Hypoxia is important in the biology and aggression of human glial brain tumors. Clin Cancer Res 10:8177–8184

[12] Powell ME, Collingridge DR, Saunders MI et al (1999) Improvement in human tumour oxygenation with carbogen of varying carbon dioxide concentrations. Radiother Oncol 50:167–171

[13] Gatenby RA, Moldofsky PJ, Weiner LM (1988) Metastatic colon cancer: correlation of oxygen levels with I-131 F(ab')2 uptake. Radiology 166:757–759

[14] Brizel DM, Scully SP, Harrelson JM et al (1996) Radiation therapy and hyperthermia improve the oxygenation of human soft tissue sarcomas. Cancer Res 56:5347–5350

[15] Pauwels EK, Mariani G (2007) Assessment of tumor tissue oxygenation: agents, methods and clinical significance. Drug News Perspect 20:619–626

[16] Massoud TF, Gambhir SS (2007) Integrating noninvasive molecular imaging into molecular medicine: an evolving paradigm. Trends Mol Med 13:183–191

[17] Willmann JK, van Bruggen N, Dinkelborg LM, Gambhir SS (2008) Molecular imaging in drug development. Nat Rev Drug Discov 7:591–607

[18] Swartz HM, Clarkson RB (1998) The measurement of oxygen *in vivo* using EPR techniques. Phys Med Biol 43:1957–1975

[19] Matsumoto K, English S, Yoo J et al (2004) Pharmacokinetics of a triarylmethyl-type paramagnetic spin probe used in EPR oximetry. Magn Reson Med 52:885–892

[20] Krohn KA, Link JM, Mason RP (2008) Molecular imaging of hypoxia. J Nucl Med 49(Suppl 2):129S–148S

[21] Wang X, Xie X, Ku G, Wang LV, Stoica G (2006) Noninvasive imaging of hemoglobin concentration and oxygenation in the rat brain using high-resolution photoacoustic tomography. J Biomed Opt 11:024015

[22] Padhani A (2010) Science to practice: what does MR oxygenation imaging tell us about human breast cancer hypoxia? Radiology 254:1–3

[23] Howe FA, Robinson SP, McIntyre DJ, Stubbs M, Griffiths JR (2001) Issues in flow and oxygenation dependent contrast (FLOOD) imaging of tumours. NMR Biomed 14:497–506

[24] Stubbs M (1999) Application of magnetic resonance techniques for imaging tumour physiology. Acta Oncol 38:845–853

[25] Tumkur SM, Vu AT, Li LP, Pierchala L, Prasad PV (2006) Evaluation of intra-renal oxygenation during water diuresis: a time-resolved study using BOLD MRI. Kidney Int 70:139–143

[26] O'Connor JP, Naish JH, Parker GJ et al (2009) Preliminary study of oxygen-enhanced longitudinal relaxation in MRI: a potential novel biomarker of oxygenation changes in solid tumors. Int J Radiat Oncol Biol Phys 75:1209–1215

[27] Mason RP (2006) Non-invasive assessment of kidney oxygenation: a role for BOLD MRI. Kidney Int 70:10–11

[28] Thomas SR, Pratt RG, Millard RW et al (1996) *In vivo* PO_2 imaging in the porcine model with perfluorocarbon F-19 NMR at low field. Magn Reson Imaging 14:103–114

[29] Mason RP, Shukla H, Antich PP (1993) *In vivo* oxygen tension and temperature: simultaneous determination using 19F NMR spectroscopy of perfluorocarbon. Magn Reson Med 29:296–302

[30] Zhao D, Ran S, Constantinescu A, Hahn EW, Mason RP (2003) Tumor oxygen dynamics: correlation of *in vivo* MRI with histological findings. Neoplasia 5:308–318

[31] van der Sanden BP, Heerschap A, Simonetti AW et al Characterization and validation of noninvasive oxygen tension measurements in human glioma xenografts by 19F-MR relaxometry. Int J Radiat Oncol Biol Phys 44:649–658

[32] McNab JA, Yung AC, Kozlowski P (2004) Tissue oxygen tension measurements in the Shionogi model of prostate cancer using 19F MRS and MRI. Magma 17:288–295

[33] Davda S, Bezabeh T (2006) Advances in methods for assessing tumor hypoxia *in vivo*: implications for treatment planning. Cancer Metastasis Rev 25:469–480

[34] Yu JX, Kodibagkar VD, Cui W, Mason RP (2005) 19F: a versatile reporter for non-invasive physiology and pharmacology using magnetic resonance. Curr Med Chem 12:819–848

[35] Hunjan S, Zhao D, Constantinescu A et al (2001) Tumor oximetry: demonstration of an enhanced dynamic mapping procedure using fluorine-19 echo planar magnetic resonance imaging in the Dunning prostate R3327-AT1 rat tumor. Int J Radiat Oncol Biol Phys 49:1097–1108

[36] Emblem KE, Mouridsen K, Bjornerud A et al (2013) Vessel architectural imaging identifies cancer patient responders to anti-angiogenic therapy. Nat Med; doi:10.1038/nm.3289

[37] Batchelor TT, Sorensen AG, di Tomaso E et al (2007) AZD2171, a pan-VEGF receptor tyrosine kinase inhibitor, normalizes tumor vasculature and alleviates edema in glioblastoma patients. Cancer Cell 11:83–95

[38] Rasey JS, Koh WJ, Evans ML et al (1996) Quantifying regional hypoxia in human tumors with positron emission tomography of [18F] fluoromisonidazole: a pretherapy study of 37 patients. Int J Radiat Oncol Biol Phys 36:417–428

[39] Lehtio K, Eskola O, Viljanen T et al (2004) Imaging perfusion and hypoxia with PET to predict radiotherapy response in head-and-neck cancer. Int J Radiat Oncol Biol Phys 59:971–982

[40] Souvatzoglou M, Grosu AL, Roper B et al (2007) Tumour hypoxia imaging with [18F] FAZA PET in head and neck cancer patients: a pilot study. Eur J Nucl Med Mol Imaging 34:1566–1575

[41] Koh WJ, Rasey JS, Evans ML et al (1992) Imaging of hypoxia in human tumors with [F-18] fluoromisonidazole. Int J Radiat Oncol Biol Phys 22:199–212

[42] Lee ST, Scott AM (2007) Hypoxia positron emission tomography imaging with 18f-fluoromisonidazole. Semin Nucl Med 37:451–461

[43] Gagel B, Reinartz P, Demirel C et al (2006) [18F] fluoromisonidazole and [18F] fluorodeoxyglucose positron emission tomography in response evaluation after chemo-/radiotherapy of non-small-cell lung cancer: a feasibility study. BMC Cancer 6:51

[44] Eschmann SM, Paulsen F, Reimold M et al (2005) Prognostic impact of hypoxia imaging with 18F-misonidazole PET in non-small cell lung cancer and head and neck cancer before radiotherapy. J Nucl Med 46:253–260

[45] Rajendran JG, Mankoff DA, O'Sullivan F et al (2004) Hypoxia and glucose metabolism in malignant tumors: evaluation by [18F] fluoromisonidazole and [18F] fluorodeoxyglucose positron emission tomography imaging. Clin Cancer Res 10:2245–2252

[46] Koh WJ, Bergman KS, Rasey JS et al (1995) Evaluation of oxygenation status during fractionated radiotherapy in human nonsmall cell lung cancers using [F-18] fluoromisonidazole positron emission tomography. Int J Radiat Oncol Biol Phys 33:391–398

[47] Rajendran JG, Wilson DC, Conrad EU et al (2003) [18F] FMISO and [18F] FDG PET imaging in soft tissue sarcomas: correlation of hypoxia, metabolism and VEGF expression. Eur J Nucl Med Mol Imaging 30:695–704

[48] Bentzen L, Keiding S, Nordsmark M et al (2003) Tumour oxygenation assessed by 18F-fluoromisonidazole PET and polarographic needle electrodes in human soft tissue tumours. Radiother Oncol 67:339–344

[49] Lehtio K, Oikonen V, Gronroos T et al (2001) Imaging of blood flow and hypoxia in head and neck cancer: initial evaluation with [15O] H_2O and [18F] fluoroerythronitroimidazole PET. J Nucl Med 42:1643–1652

[50] Yang DJ, Wallace S, Cherif A et al (1995) Development of F-18-labeled fluoroerythronitroimidazole as a PET agent for imaging tumor hypoxia. Radiology 194:795–800

[51] Barthel H, Wilson H, Collingridge DR et al (2004) *In vivo* evaluation of [18F] fluoroetanidazole as a new marker for imaging tumour hypoxia with positron emission tomography. Br J Cancer 90:2232–2242

[52] Ziemer LS, Evans SM, Kachur AV et al (2003) Noninvasive imaging of tumor hypoxia in rats using the 2-nitroimidazole 18F-EF5. Eur J Nucl Med Mol Imaging 30:259–266

[53] Evans SM, Kachur AV, Shiue CY et al (2000) Noninvasive detection of tumor hypoxia using the 2-nitroimidazole [18F] EF1. J Nucl Med 41:327–336

[54] Komar G, Seppanen M, Eskola O et al (2008) 18F-EF5: a new PET tracer for imaging hypoxia in head and neck cancer. J Nucl Med 49:1944–1951

[55] Evans SM, Fraker D, Hahn SM et al (2006) EF5 binding and clinical outcome in human soft tissue sarcomas. Int J Radiat Oncol Biol Phys 64:922–927

[56] Kumar P, Emami S, Kresolek Z et al (2009) Synthesis and hypoxia selective radiosensitization potential of beta-2-FAZA and beta-3-FAZL: fluorinated azomycin beta-nucleosides. Med Chem 5:118–129

[57] Postema EJ, McEwan AJ, Riauka TA et al (2009) Initial results of hypoxia imaging using 1-alpha-D: -(5-deoxy-5-[18F]-fluoroarabinofuranosyl)-2-nitroimidazole (18F-FAZA). Eur J Nucl Med Mol Imaging 36:1565–1573

[58] Rumsey WL, Vanderkooi JM, Wilson DF (1988) Imaging of phosphorescence: a novel method for measuring oxygen distribution in perfused tissue. Science 241:1649–1651

[59] Vinogradov SA, Grosul P, Rozhkov V et al (2003) Oxygen distributions in tissue measured by phosphorescence quenching. Adv Exp Med Biol 510:181–185

[60] Lebedev AY, Cheprakov AV, Sakadzic S et al (2009) Dendritic phosphorescent probes for oxygen imaging in biological systems. ACS Appl Mater Interfaces 1:1292–1304

[61] Pennekamp CW, Bots ML, Kappelle LJ, Moll FL, de Borst GJ (2009) The value of near-infrared spectroscopy measured cerebral oximetry during carotid endarterectomy in perioperative stroke prevention. A review. Eur J Vasc Endovasc Surg 38:539–545

[62] Jobsis FF (1977) Non-invasive, infra-red monitoring of cerebral O_2 sufficiency, blood volume, HbO_2-Hb shifts and blood flow. Acta Neurol Scand Suppl 64:452–453

[63] Hull EL, Conover DL, Foster TH (1999) Carbogen-induced changes in rat mammary tumour oxygenation reported by near infrared spectroscopy. Br J Cancer 79:1709–1716

[64] Kim JG, Liu H (2008) Investigation of biphasic tumor oxygen dynamics induced by hyperoxic gas intervention: the dynamic phantom approach. Appl Opt 47:242–252

[65] Barry BN, Mallick A, Bodenham AR, Vucevic M (1997) Lack of agreement between bioimpedance and continuous thermodilution measurement of cardiac output in intensive care unit patients. Crit Care 1:71–74

[66] Imhoff M, Lehner JH, Lohlein D (2000) Noninvasive whole-body electrical bioimpedance cardiac output and invasive thermodilution cardiac output in high-risk surgical patients. Crit Care Med 28:2812–2818

[67] Kurth CD, Steven JM, Benaron D, Chance B (1993) Near-infrared monitoring of the cerebral circulation. J Clin Monit 9:163–170

[68] Watkin SL, Spencer SA, Dimmock PW, Wickramasinghe YA, Rolfe P (1999) A comparison of pulse oximetry and near infrared spectroscopy (NIRS) in the detection of hypoxaemia occurring with pauses in nasal airflow in neonates. J Clin Monit Comput 15:441–447

[69] El-Desoky AE, Jiao LR, Havlik R, Habib N, Davidson BR, Seifalian AM (2000) Measurement of hepatic tissue hypoxia using near infrared spectroscopy: comparison with hepatic vein oxygen partial pressure. Eur Surg Res 32:207–214

[70] Fortune PM, Wagstaff M, Petros AJ (2001) Cerebro-splanchnic oxygenation ratio (CSOR) using near infrared spectroscopy may be able to predict splanchnic ischaemia in neonates. Intensive Care Med 27:1401–1407

[71] Fukui D, Urayama H, Tanaka K, Kawasaki S (2002) Use of near-infrared spectroscopic measurement at the buttocks during abdominal aortic surgery. Circ J 66:1128–1131

[72] DeBlasi RA, Quaglia E, Gasparetto A, Ferrari M (1992) Muscle oxygenation by fast near infrared spectrophotometry (NIRS) in ischemic forearm. Adv Exp Med Biol 316:163–172

[73] Shin'oka T, Nollert G, Shum-Tim D, du Plessis A, Jonas RA (2000) Utility of near-infrared spectroscopic measurements during deep hypothermic circulatory arrest. Ann Thorac Surg 69:578–583

[74] Vernieri F, Rosato N, Pauri F, Tibuzzi F, Passarelli F, Rossini PM (1999) Near infrared spectroscopy and transcranial Doppler in monohemispheric stroke. Eur Neurol 41:159–162

[75] Kurth CD, Steven JL, Montenegro LM, Watzman HM, Gaynor JW, Spray TL, Nicolson SC (2001) Cerebral oxygen saturation before congenital heart surgery. Ann Thorac Surg 72:187–192

[76] Misra M, Stark J, Dujovny M, Widman R, Ausman JI (1998) Transcranial cerebral oximetry in random normal subjects. Neurol Res 20:137–141

[77] Marik PE (2001) Sublingual capnography: A clinical validation study. Chest 120:923–927

[78] Povoas HP, Weil MH, Tang W, Sun S, Kamohara T, Bisera J (2001) Decreases in mesenteric blood flow associated with increases in sublingual pCO_2 during hemorrhagic shock. Shock 15:398–402

[79] Know, now. Sublingual CO_2. CapnoProbe Sublingual (SL) System brochure. Pleasanton, California, Nellcor Puritan Bennett, 2002, p 4

[80] Movsas B, Chapman JD, Hanlon AL, Horwitz EM, Pinover WH, Greenberg RE, Stobbe C, Hanks GE (2001) Hypoxia in human prostate carcinoma: An Eppendorf PO_2 study. Am J Clin Oncol 24:458–461

[81] Benaron DA, Parachikov IH, Friedland S et al (2004) Continuous, noninvasive, and localized microvascular tissue oximetry using visible light spectroscopy. Anesthesiology 100(6)

[82] Brun NC, Moen A, Borch K, Saugstad OD, Greisen G (1997) Near-infrared monitoring of cerebral tissue oxygen saturation and blood volume in newborn piglets. Am J Physiol 273(part 2):H682–H686

[83] Watzman HM, Kurth CD, Montenegro LM, Rome J, Steven JM, Nicolson SC (2000) Arterial and venous contributions to near-infrared cerebral oximetry. Anesthesiology 93:947–953

[84] Fantini S (2002) A haemodynamic model for the physiological interpretation of *in vivo* measurements of the concentration and oxygen saturation of haemoglobin. Phys Med Biol 47:N249–N257

[85] Maxim PG, Carson JJ, Benaron DA et al (2005) Optical detection of tumors *in vivo* by light tissue oximetry. Technol Cancer Res Treat 4:227–234.

[86] Noord DV, Sana A, Benaron DA et al (2011) Endoscopic visible light spectroscopy: a new, minimally invasive technique to diagnose chronic GI ischemia. Gastrointest Endosc 73:291–298

[87] Kaneko K, Yamaguchi H, Saito T et al (2014) Hypoxia imaging endoscopy equipped with laser light source from preclinical live animal study to first-in-human subject research. PLoS One 9(6):e99055. doi:10.1371/journal.pone.0099055

[88] Bussink J, Kaanders JH, van der Kogel AJ (2003) Tumor hypoxia at the micro-regional level: clinical relevance and predictive value of exogenous and endogenous hypoxic cell markers. Radiother Oncol 67:3–15

[89] Koukourakis MI, Bentzen SM, Giatromanolaki A et al (2006) Endogenous markers of two separate hypoxia response pathways (hypoxia inducible factor 2 alpha and carbonic anhydrase 9) are associated with radiotherapy failure in head and neck cancer patients recruited in the CHART randomized trial. J Clin Oncol 24:727–735

[90] Shibata T, Giaccia AJ, Brown JM (2000) Development of a hypoxia-responsive vector for tumor-specific gene therapy. Gene Ther 7:493–498

[91] Payen E, Bettan M, Henri A et al (2001) Oxygen tension and a pharmacological switch in the regulation of transgene expression for gene therapy. J Gene Med 3:498–504

[92] Vordermark D, Shibata T, Brown JM (2001) Green fluorescent protein is a suitable reporter of tumor hypoxia despite an oxygen requirement for chromophore formation. Neoplasia 3:527–534

[93] Harada H, Kizaka-Kondoh S, Hiraoka M (2005) Optical imaging of tumor hypoxia and evaluation of efficacy of a hypoxia-targeting drug in living animals. Mol Imaging 4:182–193

[94] Harada H, Hiraoka M, Kizaka-Kondoh S (2002) Antitumor effect of TAT-oxygen-dependent degradation-caspase-3 fusion protein specifically stabilized and activated in hypoxic tumor cells. Cancer Res 62:2013–2018

[95] Harada H, Kizaka-Kondoh S, Hiraoka M (2006) Mechanism of hypoxia-specific cytotoxicity of procaspase-3 fused with a VHL-mediated protein destruction motif of HIF-1alpha containing Pro564. FEBS Lett 580:5718–5722

[96] Harada H, Kizaka-Kondoh S, Li G et al (2007) Significance of HIF-1-active cells in angiogenesis and radioresistance. Oncogene 26:7508–7516

[97] Viola RJ, Provenzale JM, Li F et al (2008) *In vivo* bioluminescence imaging monitoring of hypoxia-inducible factor 1alpha, a promoter that protects cells, in response to chemotherapy. AJR Am J Roentgenol 191:1779–1784

[98] Mayer A, Wree A, Hockel M et al (2004) Lack of correlation between expression of HIF-1alpha protein and oxygenation status in identical tissue areas of squamous cell carcinomas of the uterine cervix. Cancer Res 64:5876–5881

[99] Lehmann S, Stiehl DP, Honer M et al (2009) Longitudinal and multimodal *in vivo* imaging of tumor hypoxia and its downstream molecular events. Proc Natl Acad Sci USA 106:14004–14009

[100] Potter CP, Harris AL (2003) Diagnostic, prognostic and therapeutic implications of carbonic anhydrases in cancer. Br J Cancer 89:2–7

[101] Ivanov S, Liao SY, Ivanova A et al (2001) Expression of hypoxia-inducible cell-surface transmembrane carbonic anhydrases in human cancer. Am J Pathol 158:905–919

[102] Wykoff CC, Beasley NJ, Watson PH et al Hypoxia-inducible expression of tumor-associated carbonic anhydrases. Cancer Res 60:7075–7083

[103] Dubois L, Lieuwes NG, Maresca A et al (2009) Imaging of CA IX with fluorescent labelled sulfonamides distinguishes hypoxic and (re)-oxygenated cells in a xenograft tumour model. Radiother Oncol 92:423–428

[104] van Dijk J, Uemura H, Beniers AJ et al Therapeutic effects of monoclonal antibody G250, interferons and tumor necrosis factor, in mice with renal-cell carcinoma xenografts. Int J Cancer 56:262–268

[105] Stillebroer AB, Oosterwijk E, Oyen WJ, Mulders PF, Boerman OC (2007) Radiolabeled antibodies in renal cell carcinoma. Cancer Imaging 7:179–188

[106] Ahlskog JK, Schliemann C, Marlind J et al (2009) Human monoclonal antibodies targeting carbonic anhydrase IX for the molecular imaging of hypoxic regions in solid tumours. Br J Cancer 101:645–657

[107] Hoogsteen IJ, Marres HA, Wijffels KI et al (2005) Colocalization of carbonic anhydrase 9 expression and cell proliferation in human head and neck squamous cell carcinoma. Clin Cancer Res 11:97–106

[108] Kim SJ, Shin HJ, Jung KY et al (2007) Prognostic value of carbonic anhydrase IX and Ki-67 expression in squamous cell carcinoma of the tongue. Jpn J Clin Oncol 37:812–819

[109] Mayer A, Hockel M, Vaupel P (2005) Carbonic anhydrase IX expression and tumor oxygenation status do not correlate at the microregional level in locally advanced cancers of the uterine cervix. Clin Cancer Res 11:7220–7225

[110] Macheda ML, Rogers S, Best JD (2005) Molecular and cellular regulation of glucose transporter (GLUT) proteins in cancer. J Cell Physiol 202:654–662

[111] Jonathan RA, Wijffels KI, Peeters W et al (2006) The prognostic value of endogenous hypoxia-related markers for head and neck squamous cell carcinomas treated with ARCON. Radiother Oncol 79:288–297

[112] Anderson RR, Parrish JA (1981) The optics of human skin. J Invest Dermat 77:13–19